Nonmonotoic fluctuation-induced interactions between dielectric slabs carrying charge disorder

Jalal Sarabadani,[1,2] Ali Naji,[3,a)] David S. Dean,[4] Ron R. Horgan,[3] and Rudolf Podgornik[2,5]

[1]*Department of Physics, University of Isfahan, Isfahan 81746, Iran*
[2]*Department of Theoretical Physics, J. Stefan Institute, SI-1000 Ljubljana, Slovenia*
[3]*Department of Applied Mathematics and Theoretical Physics, Centre for Mathematical Sciences, University of Cambridge, Cambridge CB3 0WA, United Kingdom*
[4]*Laboratoire de Physique Théorique (IRSAMC), Université de Toulouse, UPS, and CNRS, F-31062 Toulouse, France*
[5]*Department of Physics, Institute of Biophysics, and School of Medicine, Faculty of Mathematics and Physics, University of Ljubljana, SI-1000 Ljubljana, Slovenia*

We investigate the effect of monopolar charge disorder on the classical fluctuation-induced interactions between randomly charged net-neutral dielectric slabs and discuss various generalizations of recent results [A. Naji *et al.*, Phys. Rev. Lett. **104**, 060601 (2010)] to highly inhomogeneous dielectric systems with and without statistical disorder correlations. We shall focus on the specific case of two generally dissimilar plane-parallel slabs, which interact across vacuum or an arbitrary intervening dielectric medium. Monopolar charge disorder is considered to be present on the bounding surfaces and/or in the bulk of the slabs, may be in general quenched or annealed and may possess a finite lateral correlation length reflecting possible "patchiness" of the random charge distribution. In the case of quenched disorder, the bulk disorder is shown to give rise to an additive long-range contribution to the total force, which decays as the inverse distance between the slabs and may be attractive or repulsive depending on the dielectric constants of the slabs. By contrast, the force induced by annealed disorder in general combines with the underlying van der Waals forces in a nonadditive fashion, and the net force decays as an inverse cube law at large separations. We show, however, that in the case of two dissimilar slabs, the net effect due to the interplay between the disorder-induced and the pure van der Waals interactions can lead to a variety of unusual nonmonotonic interaction profiles between the dielectric slabs. In particular, when the intervening medium has a larger dielectric constant than the two slabs, we find that the net interaction can become repulsive and exhibit a potential barrier, while the underlying van der Waals force is attractive. On the contrary, when the intervening medium has a dielectric constant between that of the two slabs, the net interaction can become attractive and exhibit a free energy minimum, while the pure van der Waals force is repulsive. Therefore, the charge disorder, if present, can drastically alter the effective interaction between net-neutral objects. © *2010 American Institute of Physics*. [doi:10.1063/1.3497039]

I. INTRODUCTION

One of the most persistently made assumptions in the standard theory of (bio)colloid stability is that of a uniform charge distribution on macromolecular surfaces.[1] There are nevertheless many instances where charge patterns on macromolecular surfaces are inhomogeneous, exhibiting even a highly disordered spatial distribution. Among most notable examples are surfactant-coated surfaces[2] and random polyelectrolytes and polyampholytes.[3] The macromolecular charge pattern in these systems is often frozen, or quenched, meaning that the charge distribution does not evolve after the assembly or fabrication of the material. This is the case if the interaction between the surface charge carriers and the surfaces is of a chemical nature involving interactions that far exceed the thermal energy scale k_BT. Alternatively, charge distributions can exhibit various degrees of annealing when

interacting with other macromolecules in aqueous solutions as is, for example, the case for charge regulation of contact surfaces bearing weak acidic groups in aqueous solutions.[4]

Recently, it has also been realized that ultrahigh sensitivity experiments on Casimir (zero temperature and ideally polarizable surfaces) and van der Waals (finite temperature and nonideally polarizable surfaces) interactions between surfaces *in vacuo*[5,6] can be properly understood only if one takes into account the disordered nature of charges on and within the interacting surfaces.[6–8] Possible causes of sample- and history-specific charge disorders in this case include the patch effect, where the variation of the local crystallographic axes of the exposed surface of a clean polycrystalline sample can lead to a variation of the local surface potential.[9] Amorphous films deposited on crystalline substrates can also show a similar type of surface charge disorder, showing a grain structure of dimensions sometimes larger than the thickness of the deposited surface film.[10] On the other hand, adsorption
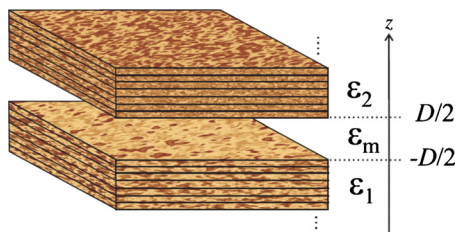
FIG. 1. We consider two semi-infinite net-neutral slabs (half-spaces) of dielectric constant ε_1 and ε_2 interacting across a medium of dielectric constant ε_m. The monopolar charge disorder (shown schematically by small light and dark patches) is distributed as random patches of finite typical size (correlation length) in a layered structure in the bulk of the slabs and on the two bounding surfaces at $z = \pm D/2$. It may be either quenched or annealed.

of various contaminants can influence the nature and type of the surface charge disorder.

Since the nature and distribution of the charge disorder in any of the force experiments are in general seldom known, we pursue a strategy of assessing the consequences of different *a priori* models of the distribution of charge disorder. In what follows, we will thus assume that the charge disorder stems from randomly distributed *monopolar charges*, which may be present both in the bulk and/or on the interacting surfaces and can be either annealed or quenched. In the quenched case, the disorder charges are frozen, whereas in the annealed case, the disorder charges are subject to thermal fluctuations at ambient temperature and can thus adapt themselves in order to minimize the free energy of the system. We do not deal with effects due to disorder in the dielectric response of the interacting media,[11] which presents an additional source of disorder meriting further study. We have shown in our previous works[8,12,13] that the type and the nature of the charge disorder induce marked changes in the properties of the total interaction between apposed bodies and the force arising from the presence of disordered charges can dominate the underlying Casimir–van der Waals (vdW) effect at sufficiently large separations. The analysis of the *interaction fingerprint* of the charge disorder can be useful in assessing whether the experimentally observed interactions can be interpreted in terms of disorder effects or are due to pure Casimir–vdW interactions. In this study, we will continue with the assessment of this interaction fingerprint in the case of two semi-infinite net-neutral dielectric slabs (separated by a layer of vacuum or an arbitrary unstructured dielectric material as shown in Fig. 1) by generalizing our formalism to include two different mechanisms.

(i)   The "patchy" distribution of the charge disorder, which may arise due to finite correlations between the carriers of the charge disorder. This is a rather realistic assumption in view of the graininess observed in interacting surfaces.[9,10]

(ii)   The dielectric inhomogeneity effects in highly asymmetric systems, where the two slabs and the intervening medium may in general have different dielectric properties.

For interacting bodies carrying no *net* charge, the part of the interaction due to monopolar *quenched charge* disorder can be seen from a full quantum field-theoretical formalism[14]

to be coupled directly to the zero-frequency or *classical* vdW interaction (corresponding to the zero-frequency Matsubara modes of the electromagnetic field). The situation would be more complicated in the case of annealed disorder if one is to account for the higher-order Matsubara frequencies and a general treatment is missing at present. In this work, we shall examine the effects of quenched and annealed charge disorder by focusing specifically on the zero-frequency vdW interaction. It is well known that the higher frequency Matsubara terms in the total vdW interaction free energy become relatively unimportant at sufficiently high temperatures and/or sufficiently large intersurface separations.[5] In this paper, we will restrict ourselves to this regime, which is also most relevant experimentally[6] and consider the short-distance quantum effects elsewhere.[14]

As we shall demonstrate, the interplay and competition of the underlying vdW effect between the two semi-infinite slabs and the interaction induced by the charge disorder can give rise to a variety of different interaction profiles, including, most notably, *nonmonotonic* interactions as a function of the interslab distance. In particular, when the two dielectrics interact across a medium of higher dielectric constant, the disorder force can become strongly repulsive and thus generate a potential barrier when combined with the vdW force, which is attractive in that case. While, in the situation where the intervening medium has a dielectric constant in between that of the two slabs,[15] the disorder can generate an attractive force, which can balance the repulsive vdW force, leading thus to a stable bound state between the two dielectric slabs. Therefore, the charge disorder, if present, can provide an intrinsic mechanism to stabilize interactions between net-neutral bodies. These features emerge because the disorder-induced interactions typically decay more weakly with the separation than the vdW interaction and depend strongly on the dielectric inhomogeneities in the system.

The above features vary depending on whether the disorder is assumed to be quenched or annealed. The effects due to annealed charge disorder can be distinctly different from those of the quenched charge disorder. In the case of annealed charges, the effective interactions turn out to decay more rapidly and in fact in a similar way as the pure vdW interaction, whereas in the case of quenched charges, the net interactions decay more weakly with the separation, i.e., as $\sim D^{-\alpha}$, where $\alpha = 1$ if the disorder is present in the bulk of the slabs and $\alpha = 2$ if the disorder is confined to the bounding surfaces of the slabs.

The organization of the paper is as follows. In Sec. II, we introduce the details of our model and the formalism used in our study. The general results are derived in Secs. III A and III B for the case of quenched and annealed disorders, respectively. We shall proceed with the analysis of the effective interaction between two identical slabs in Sec. IV, where we shall focus mainly on the effects due to spatial correlation in the distribution of the charge disorder. In Sec. V, we study the interaction in dielectrically asymmetric systems by considering two dissimilar dielectric slabs that interact across an arbitrary dielectric medium. The results and limitations of our study are summarized in Sec. VI.

II. MODEL

Let us consider two semi-infinite slabs of dielectric constants ε_1 and ε_2 and temperature T with parallel planar inner surfaces (of infinite area S) located normal to the z axis at $z = \pm D/2$ (see Fig. 1). The inner gap is filled with a material of dielectric constant ε_m. The inhomogeneous dielectric constant profile for this system is thus given by

$$\varepsilon(\mathbf{r}) = \begin{cases} \varepsilon_1 & z < -D/2 \\ \varepsilon_m & |z| < D/2 \\ \varepsilon_2 & z > D/2. \end{cases} \quad (1)$$

We shall assume that the two dielectric slabs have a disordered monopolar charge distribution, $\rho(\mathbf{r})$, which may arise from randomly distributed charges residing on the bounding surfaces [$\rho_s(\mathbf{r})$] and/or in the bulk [$\rho_b(\mathbf{r})$], i.e., $\rho(\mathbf{r}) = \rho_s(\mathbf{r}) + \rho_b(\mathbf{r})$. The charge disorder is assumed to be distributed according to a Gaussian weight with zero mean (i.e., the slabs are *net-neutral*) and the two-point correlation function[16]

$$\langle\langle \rho(\mathbf{r})\rho(\mathbf{r}') \rangle\rangle = \mathcal{G}(\boldsymbol{\varrho} - \boldsymbol{\varrho}'; z)\delta(z - z'), \quad (2)$$

where $\langle\langle \cdots \rangle\rangle$ denotes the average over all realizations of the charge disorder distribution, $\rho(\mathbf{r})$. We have thus assumed that there are no spatial correlations in the *perpendicular* direction, z; however, in the *lateral* directions $\boldsymbol{\varrho} = (x, y)$ (in the plane of the dielectrics), we have a finite statistically invariant correlation function whose specific form may depend on z as well. This implies that the charge disorder is distributed in general as random "patches" in a layered structure in the bulk of the slabs as well as on the bounding surfaces.

The total correlation function can be written as the sum of the surface (s) and bulk (b) contributions,

$$\mathcal{G}(\boldsymbol{\varrho} - \boldsymbol{\varrho}'; z) = g_s(z)c_s(\boldsymbol{\varrho} - \boldsymbol{\varrho}'; z) + g_b(z)c_b(\boldsymbol{\varrho} - \boldsymbol{\varrho}'; z). \quad (3)$$

For the slab geometry, we generally assume that the lateral correlation functions may be different for the two slabs, i.e.,

$$c_s(\mathbf{x}; z) = \begin{cases} c_{1s}(\mathbf{x}) & z = -D/2 \\ c_{2s}(\mathbf{x}) & z = D/2, \end{cases} \quad (4)$$

$$c_b(\mathbf{x}; z) = \begin{cases} c_{1b}(\mathbf{x}) & z < -D/2 \\ 0 & |z| < D/2 \\ c_{2b}(\mathbf{x}) & z > D/2, \end{cases} \quad (5)$$

and that the surface and bulk variances are given by

$$g_s(z) = e_0^2[g_{1s}\delta(z + D/2) + g_{2s}\delta(z - D/2)], \quad (6)$$

$$g_b(z) = \begin{cases} g_{1b}e_0^2 & z < -D/2 \\ 0 & |z| < D/2 \\ g_{2b}e_0^2 & z > D/2. \end{cases} \quad (7)$$

The lateral correlation between two given points is typically expected to decay with their separation over a finite *correlation length* ("patch size"), which could in general be highly material or sample specific. However, the main aspects of the patchy structure of the disorder can be investigated by assuming simple generic models with, for instance,

a Gaussian or an exponentially decaying correlation function. Without loss of generality, we shall choose an exponentially decaying correlation function according to the two-dimensional Yukawa form,[17]

$$c_{i\alpha}(\mathbf{x}) = \frac{1}{2\pi\xi_{i\alpha}^2}K_0\left(\frac{|\mathbf{x}|}{\xi_{i\alpha}}\right), \quad (8)$$

where $\xi_{i\alpha}$ represents the correlation length for the bulk or surface disorder ($\alpha = b, s$) in the ith slab ($i = 1, 2$). The case of a completely *uncorrelated* disorder[8] follows as a special case for $\xi_{i\alpha} \to 0$ from our formalism. We should emphasize that the correlation assumed for the bulk disorder is only present in the plane of the slab surfaces and not in the direction perpendicular to them. This assumption is wholly justified only for *layered materials*. In all the other cases of the bulk disorder, one would normally expect the same correlation length in the direction perpendicular to the surfaces. We will deal with this model in a separate publication.

III. FORMALISM

The partition function for the classical vdW interaction (the zero-frequency Matsubara modes of the electromagnetic field) may be written as a functional integral over the scalar field $\phi(\mathbf{r})$,

$$\mathcal{Z}[\rho(\mathbf{r})] = \int [\mathcal{D}\phi(\mathbf{r})]e^{-\beta\mathcal{S}[\phi(\mathbf{r}); \rho(\mathbf{r})]}, \quad (9)$$

with $\beta = 1/k_\mathrm{B}T$ and the effective action

$$\mathcal{S}[\phi(\mathbf{r}); \rho(\mathbf{r})] = \int d\mathbf{r}\left[\frac{1}{2}\varepsilon_0\varepsilon(\mathbf{r})(\nabla\phi(\mathbf{r}))^2 + i\rho(\mathbf{r})\phi(\mathbf{r})\right]. \quad (10)$$

The above partition function can be used to evaluate averaged quantities such as the effective interaction between the dielectric bodies. However, since the charge distribution, $\rho(\mathbf{r})$, is disordered, it is necessary to average the partition function over different realizations of the charge distribution. The averaging procedure differs depending on the nature of the disorder. In what follows, we consider two idealized cases of either completely quenched or completely annealed disorder[18] (the intermediate case of partially annealed disorder is also analytically tractable[13] but will not be considered here).

A. Correlated quenched disorder

The quenched disorder corresponds to the situation where the disorder charges are frozen and cannot fluctuate and equilibrate with other degrees of freedom in the system. As it is well known, the disorder average in this case must be taken over the sample free energy, $\ln \mathcal{Z}[\rho(\mathbf{r})]$, in order to evaluate the averaged quantities.[18] Therefore, the free energy of the quenched model is given by

$$\beta\mathcal{F}_{\mathrm{quenched}} = -\langle\langle \ln \mathcal{Z}[\rho(\mathbf{r})]\rangle\rangle. \quad (11)$$

The Gaussian integral in Eq. (9) as well as the disorder average can be evaluated straightforwardly in this case, yielding[16]

$$\beta\mathcal{F}_{\text{quenched}} = \frac{1}{2}\text{Tr}\ln G^{-1}(\mathbf{r},\mathbf{r}')$$
$$+ \frac{\beta}{2}\int d\mathbf{r}d\mathbf{r}'\mathcal{G}(\boldsymbol{\varrho}-\boldsymbol{\varrho}';z)\delta(z-z')G(\mathbf{r},\mathbf{r}'),$$
$$(12)$$

where $G(\mathbf{r},\mathbf{r}')$ is the Green's function defined via

$$\varepsilon_0\nabla\cdot[\varepsilon(\mathbf{r})\nabla G(\mathbf{r},\mathbf{r}')] = -\delta(\mathbf{r}-\mathbf{r}'). \qquad (13)$$

Note that the free energy (12) of the quenched model is expressed in terms of different additive contributions, i.e.,

$$\mathcal{F}_{\text{quenched}} = \mathcal{F}_{\text{vdW}} + \mathcal{F}_b + \mathcal{F}_s. \qquad (14)$$

The first term above is nothing but the usual contribution from the zero-frequency vdW interaction,

$$\beta\mathcal{F}_{\text{vdW}} = \frac{1}{2}\text{Tr}\ln G^{-1}(\mathbf{r},\mathbf{r}'), \qquad (15)$$

which is always present between neutral dielectrics even in the absence of any monopolar charge disorder. The second and the third terms represent contributions from the bulk and surface disorder ($\alpha = b,s$),

$$\beta\mathcal{F}_{\alpha} = \frac{\beta}{2}\int d\mathbf{r}d\mathbf{r}'g_{\alpha}(z)c_{\alpha}(\boldsymbol{\varrho}-\boldsymbol{\varrho}';z)\delta(z-z')G(\mathbf{r},\mathbf{r}'). \qquad (16)$$

The quenched expression (12) is valid for any arbitrary disorder correlation function $\mathcal{G}(\boldsymbol{\varrho}-\boldsymbol{\varrho}';z)$ and dielectric constant profile $\varepsilon(\mathbf{r})$. In what follows, we shall focus on the particular case of planar dielectrics by employing Eqs. (1) and (3)–(7). In this case, the zero-frequency vdW contribution is obtained (per k_BT and unit area) as[5]

$$\frac{\beta\mathcal{F}_{\text{vdW}}}{S} = \frac{1}{2}\int\frac{d^2Q}{(2\pi)^2}\ln(1-\Delta_1\Delta_2 e^{-2QD}). \qquad (17)$$

The force associated with this contribution, $f_{\text{vdW}} = -\partial\mathcal{F}_{\text{vdW}}/\partial D$, follows as

$$\frac{\beta f_{\text{vdW}}}{S} = -\frac{\text{Li}_3(\Delta_1\Delta_2)}{8\pi D^3}. \qquad (18)$$

The dielectric jump parameters are defined as

$$\Delta_i = \frac{\varepsilon_i - \varepsilon_m}{\varepsilon_i + \varepsilon_m} \qquad (19)$$

at each of the bounding surfaces ($i=1,2$), and $\text{Li}_3(\cdot)$ is the trilogarithm function defined by

$$\text{Li}_3(z) = \sum_{n=1}^{\infty}\frac{z^n}{n^3}. \qquad (20)$$

The dielectric constants of the system enter the expression (17) via the terms Δ_1 and Δ_2. If $\Delta_1\Delta_2 > 0$, then the vdW interaction between the slabs is attractive; otherwise, the vdW force is repulsive.

The expression in Eq. (16) can be calculated in a straightforward manner. We obtain the bulk disorder contribution as

$$\frac{\beta\mathcal{F}_b}{S} = -\ell_B\varepsilon_m\int\frac{dQ}{Q}\frac{e^{-2QD}}{1-\Delta_1\Delta_2 e^{-2QD}}\left[\frac{g_{1b}c_{1b}(Q)}{(\varepsilon_1+\varepsilon_m)^2}\Delta_2\right.$$
$$\left. + \frac{g_{2b}c_{2b}(Q)}{(\varepsilon_2+\varepsilon_m)^2}\Delta_1\right], \qquad (21)$$

and the surface disorder contribution as

$$\frac{\beta\mathcal{F}_s}{S} = -2\ell_B\varepsilon_m\int dQ\frac{e^{-2QD}}{1-\Delta_1\Delta_2 e^{-2QD}}$$
$$\times\left[\frac{g_{1s}c_{1s}(Q)}{(\varepsilon_1+\varepsilon_m)^2}\Delta_2 + \frac{g_{2s}c_{2s}(Q)}{(\varepsilon_2+\varepsilon_m)^2}\Delta_1\right], \qquad (22)$$

at all separations D, where

$$\ell_B = \beta e_0^2/(4\pi\varepsilon_0) \qquad (23)$$

is the Bjerrum length in vacuum ($\ell_B \simeq 56.8$ nm at room temperature) and $c_{i\alpha}(Q)$ is the Fourier transform of the correlation function $c_{i\alpha}(\mathbf{x})$. For the particular form of $c_{i\alpha}(\mathbf{x})$ chosen in Eq. (8), we have a Lorentzian Fourier transform (for $i=1,2$ and $\alpha=b,s$) as

$$c_{i\alpha}(Q) = \frac{1}{\xi_{i\alpha}^2 Q^2 + 1}. \qquad (24)$$

The total force between the dielectric slabs carrying quenched charge disorder thus follows from $f_{\text{quenched}} = -\partial\mathcal{F}_{\text{quenched}}/\partial D$ and the preceding free energy expressions as

$$\frac{\beta f_{\text{quenched}}}{S} = -\frac{\text{Li}_3(\Delta_1\Delta_2)}{8\pi D^3} - 2\ell_B\varepsilon_m$$
$$\times\int_0^{\infty}\frac{dQe^{-2QD}}{(1-\Delta_1\Delta_2 e^{-2QD})^2}\left[\frac{g_{1b}c_{1b}(Q)}{(\varepsilon_1+\varepsilon_m)^2}\Delta_2\right.$$
$$+ \frac{g_{2b}c_{2b}(Q)}{(\varepsilon_2+\varepsilon_m)^2}\Delta_1 + \frac{2Qg_{1s}c_{1s}(Q)}{(\varepsilon_1+\varepsilon_m)^2}\Delta_2$$
$$\left. + \frac{2Qg_{2s}c_{2s}(Q)}{(\varepsilon_2+\varepsilon_m)^2}\Delta_1\right]. \qquad (25)$$

We notice that the quenched disorder contribution to the force has a number of interesting features. We see that the forces generated due to the charge disorder in slab 1 and slab 2 are independent and additive. If we remove the charge disorder from either slab, we see that there is still a contribution coming from the other slab. This is because the charge distributions on average do not interact with each other. As the charge distribution in opposing slabs is uncorrelated, the average force on a charge in slab 1 due to a charge in slab 2 is zero as the charge in slab two is equally likely to have a positive charge as a negative charge. In fact, the charges in slab 1 are only correlated with their *image charges* in slab 2; this means that on average the charge distribution in slab 1 only interacts with its image in slab 2 and vice versa. The *sign* of the interaction between charges in slab 1 and their images in slab 2 depends on Δ_2. If Δ_2 is positive, that is, the dielectric constant of slab 2 is greater than that of the intervening material, $\varepsilon_2 > \varepsilon_m$, then the force due to the charge in slab 1 is attractive. Therefore, the contribution of the charge in each slab to the net force depends on the dielectric con-

trast between the opposing slab and the intervening medium. Thus, while the vdW contribution depends on the product $\Delta_1\Delta_2$, the contribution from the quenched charge distribution in slab 1 depends on variance $g_{1s,b}$ of the charge on the surface or bulk of this slab but on Δ_2 of the slab 2. This leads to a rich phenomenology of possible net interactions. For example, if Δ_1 and Δ_2 are both positive, the vdW force is attractive and so are the forces due to both charge distributions. However, if Δ_1 and Δ_2 are negative, the vdW force is again attractive, but the force due to both quenched charge distributions is repulsive. Also, note that while the vdW term shows a standard $1/D^3$ decay with the surface separation D, the disorder contribution turns out to have a much weaker decay with the separation[8] as we shall analyze further in the forthcoming sections. Therefore, the interplay between these different contributions can lead to characteristically different interaction profiles depending on the system parameters.

B. Correlated annealed disorder

In the annealed model, disorder charges are assumed to fluctuate in thermal equilibrium with the rest of the system, and thus, in particular, the charge distribution in the two slabs can adapt itself to minimize the free energy of the system. In this case, the disorder degrees of freedom should be treated statistically on the same footing as other degrees of freedom, which implies that the disorder average must be taken over the sample partition function $\mathcal{Z}[\rho(\mathbf{r})]$.[18] Hence, the free energy of the annealed model reads

$$\beta\mathcal{F}_{\text{annealed}} = -\ln\langle\langle \mathcal{Z}[\rho(\mathbf{r})]\rangle\rangle. \tag{26}$$

The annealed free energy may be evaluated using Eqs. (2), (9), and (26) as

$$\beta\mathcal{F}_{\text{annealed}} = \tfrac{1}{2}\text{Tr}\,\ln[G^{-1}(\mathbf{r},\mathbf{r}') + \beta\mathcal{G}(\boldsymbol{\varrho}-\boldsymbol{\varrho}';z)\delta(z-z')]. \tag{27}$$

Note that unlike the quenched case, Eq. (12), the disorder contributions cannot be in general separated from the pure vdW contribution when the disorder is annealed.

In the case of two interacting planar dielectrics, we shall make use of Eqs. (1) and (3)–(7) in order to calculate the fluctuational trace-log of the modified inverse Green's function $G^{-1}(\mathbf{r},\mathbf{r}')+\beta\mathcal{G}(\boldsymbol{\varrho}-\boldsymbol{\varrho}';z)\delta(z-z')$ in Eq. (27). By employing standard procedures,[19] we find

$$\frac{\beta\mathcal{F}_{\text{annealed}}}{S} = \frac{1}{2}\int \frac{\mathrm{d}^2Q}{(2\pi)^2}\ln[1 - \Delta_{1g}(Q)\Delta_{2g}(Q)e^{-2QD}], \tag{28}$$

where we have (for $i=1,2$)

$$\Delta_{ig}(Q) = \frac{\varepsilon_m Q - \varepsilon_i\sqrt{Q^2 + 4\pi\ell_{\text{B}}g_{ib}c_{ib}(Q)/\varepsilon_i} - 4\pi\ell_{\text{B}}g_{is}c_{is}(Q)}{\varepsilon_m Q + \varepsilon_i\sqrt{Q^2 + 4\pi\ell_{\text{B}}g_{ib}c_{ib}(Q)/\varepsilon_i} + 4\pi\ell_{\text{B}}g_{is}c_{is}(Q)}. \tag{29}$$

The total force, $f_{\text{annealed}} = -\partial\mathcal{F}_{\text{annealed}}/\partial D$, in the annealed model thus follows as

$$\frac{\beta f_{\text{annealed}}}{S} = -\frac{1}{2\pi}\int Q^2\mathrm{d}Q \frac{\Delta_{1g}(Q)\Delta_{2g}(Q)e^{-2QD}}{1 - \Delta_{1g}(Q)\Delta_{2g}(Q)e^{-2QD}}. \tag{30}$$

The annealed interaction free energy, or the corresponding force, has a form reminiscent of the zero-frequency vdW interaction between two semi-infinite slabs[20] with renormalized dielectric mismatch, $\Delta_{ig}(Q)$, depending on the in-plane wave-vector Q. Indeed, one can argue for the following exact correspondence based on the vdW interactions between media with volume and surface embedded mobile charges:[20,21] the term $\sqrt{Q^2+4\pi\ell_{\text{B}}g_{ib}c_{ib}(Q)/\varepsilon_i}$ corresponds to bulk Debye-like "screening," stemming from the annealed bulk disorder response to local electrostatic fields. It can be obtained alternatively by analyzing the fluctuational modes of the Debye–Hückel fields as opposed to the Laplace fields.[20] The term $4\pi\ell_{\text{B}}g_{is}c_{is}(Q)$, on the other hand, stems from the response of the mobile charges confined to the dielectric surfaces to electrostatic fields, corresponding to surface disorder-generated screening.[21] It can be derived alternatively by considering the response of the surface polarization to local electrostatic fileds.[21] The combination of the two terms in Eq. (30) cannot be written as a sum of two terms depending linearly on c_{ib} and c_{is}. This signifies that the bulk and surface disorder effects for the annealed case are obviously not additive and cannot be analyzed separately.

Note also that the case of an uncorrelated annealed disorder ($c_{ib}, c_{is} = 1$) corresponds exactly to the situation where the semi-infinite slabs are considered to be composed of a free Debye–Hückel plasma of positive and negative charges at equilibrium.[22] A nontrivial correlation function as we use here can be obtained for such a plasma only in the presence of an underlying non-Coulombic interaction of the mobile ions with, e.g., impurities that induces such correlations in the distribution of the ions.[17]

IV. SYMMETRIC CASE OF TWO IDENTICAL SLABS

We now analyze the preceding analytical results in the situation where the two dielectric slabs are identical, i.e., we have $\varepsilon_i = \varepsilon_p$ ($\Delta_i = \Delta$), $g_{is} = g_s$, $g_{ib} = g_b$, and $\xi_{is} = \xi_{ib} = \xi$ for both slabs $i=1,2$.

A. Quenched disorder-induced interactions

In the case of quenched disorder, one can expand the Lorentzian correlation function $c_{i\alpha}(Q)$, Eq. (24), in powers of the dimensionless ratio of the correlation length to the intersurface separation, ξ/D, and thus express the total force (25) in the form of a series expansion as

$$f_{\text{quenched}} = f^{(0)} + \sum_{n=1}^{\infty} f^{(n)}, \tag{31}$$

where the leading order term

$$\frac{\beta f^{(0)}}{S} = -\frac{g_b\ell_{\text{B}}\Delta}{2\varepsilon_p D} - \frac{2\varepsilon_m g_s\ell_{\text{B}}|\ln(1-\Delta^2)|}{(\varepsilon_m + \varepsilon_p)^2\Delta D^2} - \frac{\text{Li}_3(\Delta^2)}{8\pi D^3}, \tag{32}$$

corresponds to the free energy of the system in the presence of a completely uncorrelated disorder ($\xi=0$),[8] and the higher-

order terms that stem from the lateral disorder correlations follow as

$$\frac{\beta f^{(n)}}{S} = -\frac{4g_b\ell_B\varepsilon_m}{(\varepsilon_m+\varepsilon_p)^2\Delta D}\sum_{n=1}^{\infty}(-1)^n\frac{\xi^{2n}}{D^{2n}}C_{2n+1}\mathrm{Li}_{2n}(\Delta^2)$$
$$-\frac{8g_s\ell_B\varepsilon_m}{(\varepsilon_m+\varepsilon_p)^2\Delta D^2}\sum_{n=1}^{\infty}(-1)^n\frac{\xi^{2n}}{D^{2n}}C_{2n+2}\mathrm{Li}_{2n+1}(\Delta^2),$$

$$(33)$$

where $C_n=\Gamma(n)/2^n$. The above series expansion is most suitable for the situation where ξ/D is small.

Let us first consider the leading order uncorrelated disorder free energy $f^{(0)}$ in Eq. (32). This contribution exhibits a few remarkable features.[8] First, it shows a sequence of scaling behaviors with the separation that stem from different origins: a leading $1/D$ term due to the quenched bulk disorder, a subleading $1/D^2$ term from the surface charge disorder, and the pure vdW term that goes as $1/D^3$, i.e.,

$$\frac{\beta f_{\mathrm{vdW}}}{S} = -\frac{\mathrm{Li}_3(\Delta^2)}{8\pi D^3}.$$

$$(34)$$

While the vdW term is always attractive in a symmetric system, the disorder contributions [first and second terms in Eq. (32)] are attractive when the dielectric mismatch $\Delta>0$ (i.e., when the dielectric constant of the intervening medium is smaller than that of the slabs) and repulsive otherwise. The former case ($\Delta>0$) has been investigated in detail previously in the context of two identical dielectric slabs in vacuum ($\varepsilon_m=1$).[8]

Note that since the forces induced by an uncorrelated disorder exhibit a much weaker decay with the separation, they may completely mask the standard vdW force (which is always present regardless of any charge disorder) at sufficiently large separations.[8] One might expect that globally electroneutral slabs would exhibit a dipolarlike interaction force to the leading order rather than the monopolar forms $1/D$ (or $1/D^2$) obtained for the bulk (or surface) charge distribution. As noted before, the physics involved is indeed subtle as the disorder terms result from the self-interaction of the charges with their images [which follows from $G(\mathbf{r},\mathbf{r})$, Eq. (12), in the limit of zero correlation length] and not from dipolar interactions [which come from an expansion of $G(\mathbf{r},\mathbf{r}')$ when $|\mathbf{r}-\mathbf{r}'|$ is large]. Statistically speaking, each charge on average (as any other charge has an equal probability of being of the same or opposite sign) only sees its image, thus explaining the leading monopolar form in the net force.[23]

Note that the above discussion holds at separations much larger than the correlation length ξ (corresponding to small patch size compared to the separation distance D), where the disorder can be considered effectively to be statistically uncorrelated. At smaller separations (or for larger correlations lengths), one must take into account the higher-order corrections as well. The next leading correction due to disorder correlations for small ξ/D follows from Eq. (33) as
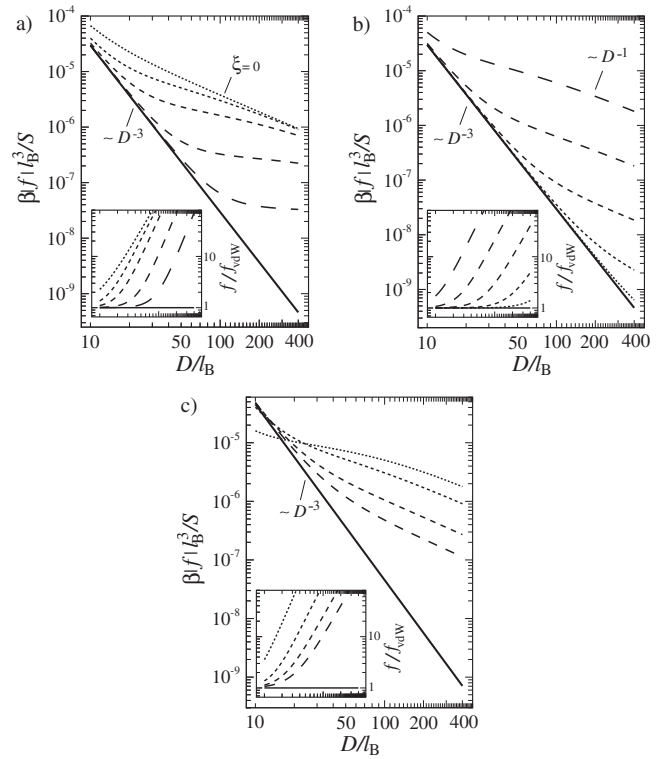

FIG. 2. (a) Magnitude of the rescaled total force, $\beta|f|l_B^3/S$ [Eq. (25)], between two identical net-neutral dielectric slabs in *vacuum* ($\varepsilon_m=1$) bearing *quenched* monopolar charge disorder as a function of the rescaled distance, D/l_B. The results are plotted here for fixed $\varepsilon_p=10$, $g_s=0$ (no surface disorder) and bulk disorder variance $g_b=5\times10^{-8}$ nm^{-3}, and varying disorder correlation lengths $\xi/l_B=0$, 200, 10^3, 10^4, and 10^5 (from top to bottom). Inset shows the ratio of the total force to the pure zero-frequency vdW force (34) between the slabs in the absence of charge disorder for the same range of D. (b) Same as (a) but here we fix $\varepsilon_p=10$, $g_s=0$, and $\xi/l_B=200$ and vary the bulk disorder variance in the range $g_b=10^{-7}$, 10^{-8}, 10^{-9}, 10^{-10}, and 10^{-11} nm^{-3} (from top to bottom). Solid curve is the pure vdW force (34). (c) Same as (b) but here we fix $\xi/l_B=200$, $g_b=5\times10^{-8}$ nm^{-3}, and $g_s=g_b^{2/3}$ and vary the dielectric constant of slabs as $\varepsilon_p=2$ (top dotted curve), 10, 40, and 100 (bottom dot-dashed curve). All graphs are plotted in log-log scale.

$$\frac{\beta f^{(1)}}{S} \simeq \frac{g_b\ell_B\varepsilon_m\xi^2\mathrm{Li}_2(\Delta^2)}{(\varepsilon_p+\varepsilon_m)^2\Delta D^3} + \frac{3\varepsilon_mg_s\ell_B\xi^2\mathrm{Li}_3(\Delta^2)}{(\varepsilon_m+\varepsilon_p)^2\Delta D^4},$$

$$(35)$$

which has an opposite sign to the zeroth-order term and thus tends to weaken the zeroth-order effect. Note however that the higher-order corrections in Eq. (33) alternatively change sign and their net effect leads to a total force, which can be evaluated numerically, e.g., directly from Eq. (25). The results are shown in Fig. 2 for the case of two identical dielectric slabs in vacuum. As seen in Fig. 2(a), the attractive disorder-induced forces indeed diminish (albeit rather slowly as seen in the inset) as the disorder correlation length is increased (by several orders of magnitude from $\xi=0$ up to $\xi\simeq5$ mm in actual units in the figure). For a large correlation length or at small separation (large ξ/D), the total force thus tends to the nondisordered vdW force (34) that scales as $1/D^3$ (thick solid line), while for a small correlation length or at large separation (small ξ/D), the force increases and shows a crossover to the maximal uncorrelated disorder value (32) that scales as $1/D$ (top dotted line). The latter is obviously from the bulk disorder, which, if present, gives rise to the most dominant effects.
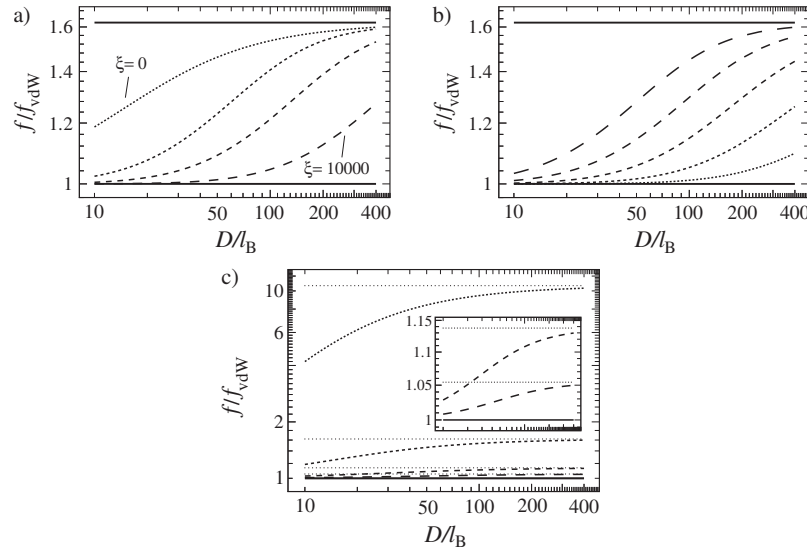
FIG. 3. (a) Ratio of the total force (30) to the zero-frequency vdW force (34) between two identical net-neutral dielectric slabs in vacuum ($\varepsilon_m=1$) bearing *annealed* monopolar charge disorder as a function of the rescaled distance, D/l_B. The results are plotted here for fixed $\varepsilon_p=10$, $g_s=0$ (no surface disorder), $g_b=5\times10^{-8}$ nm^{-3}, and varying disorder correlation length $\xi/l_B=0$, 200, 10^3, and 10^4 (from top to bottom). Annealed curves are bounded by the perfect conductor result, Eq. (37) (top solid line), for large disorder and the vdW result, Eq. (34) (bottom solid line), for no disorder. (b) Same as (a) but here we have fixed $\varepsilon_p=10$, $g_s=0$, $\xi/l_B=200$, and bulk disorder variance varied in the range $g_b=10^{-7}$, 10^{-8}, 10^{-9}, 10^{-10}, and 10^{-11} nm^{-3} (from top to bottom). (c) Same as (a) but here we fix $g_s=0$, $g_b=5\times10^{-8}$ nm^{-3}, and $\xi=0$ and vary the dielectric constant of the slabs as $\varepsilon_p=2$, 10, 40, and 100 (from top). Inset shows a closer view of the curves for $\varepsilon_p=40$ and 100 (from top). Top dotted lines correspond to Eq. (37). All graphs are plotted in log-log scale.

The crossover behavior depends also significantly on the disorder variance and the dielectric mismatch [Figs. 2(b) and 2(c)]. Similar trends as described above can be observed by varying the bulk disorder variance, g_b, as shown in Fig. 2(b) (here, g_b varies within the typical range[24] of $10^{-11}-10^{-7}$ nm^{-3}, corresponding to impurity charge densities of $10^{10}-10^{14}$ e_0/cm^3). The results in Fig. 2(c), however, reveal a nonmonotonic dependence on the dielectric mismatch. The disorder contribution tends to decrease both for small and large slab dielectric constant. This can be seen directly from Eqs. (32) and (33) as the disorder-induced force vanishes in the limits $\varepsilon_p\to\infty$ or $\Delta\to1$ (perfect conductor) and $\Delta\to0$ (homogeneous medium, in which case the vdW force vanishes as well).

It is interesting to note that the first-order corrections due to *bulk correlations* scales in the dipolar form as $1/D^3$, which is similar to the vdW contribution. Hence, these corrections tend to renormalize the ideal zero-frequency Hamaker coefficient, $A\equiv3(k_BT)Li_3(\Delta^2)/4$, associated with the vdW term [defined via $f_{vdW}/S=-A/(6\pi D^3)$] to an effective value given by

$$A_{eff}=\frac{3k_BT}{4}Li_3(\Delta^2)-\frac{3g_be_0^2\varepsilon_m\xi^2Li_2(\Delta^2)}{2\varepsilon_0(\varepsilon_p+\varepsilon_m)^2\Delta}.\qquad(36)$$

This value is smaller (larger) than the ideal value A when $\Delta>0$ ($\Delta<0$) and can even change sign.

B. Annealed disorder-induced interactions

In the case of annealed disorder, the total force between the dielectric slabs is given by Eq. (30). It shows that the force in this case cannot be expressed simply as a sum of different additive contributions as in the quenched case. Rather, it follows from the combined effect of the annealed disorder fluctuations and the underlying vdW effect, which again reflects the fact that the disorder charge distribution in this case can adapt itself in order to minimize the total free energy of the system.

The resulting total force is shown in Fig. 3 for the symmetric case of two identical dielectric slabs in vacuum. For the sake of presentation, we have plotted the ratio of the annealed force (30) to the vdW force (34), which clearly shows that the net force is bounded by two *limiting laws*, namely, the ideal limiting force

$$\frac{\beta f_{ideal}}{S}=-\frac{\zeta(3)}{8\pi D^3},\qquad(37)$$

which is similar to the one obtained between perfect conductors[5] and the vdW force (34) in the absence of any disorder charges. These constitute the upper and the lower bounds for the annealed force in the general symmetric case with $\Delta>0$, i.e.,

$$|f_{vdW}|<|f_{annealed}|<|f_{ideal}|.\qquad(38)$$

Note that the above limiting values can be established systematically from the general expression (30) and are strictly attractive (negative sign). The lower bound vdW force is nonuniversal (i.e., material dependent) and is obtained asymptotically in the limit of small disorder variance (g_b, $g_s\to0$) or small separations. The upper bound is *universal* and follows in the limit of strong disorder variance (g_b or $g_s\to\infty$) or large separations. The crossover from one limit to the other can be achieved by increasing the distance or the disorder variance as seen in Fig. 3.

In general, the net interaction forces in the annealed case turn out to decay more strongly with the slab separation distance as compared with the case of quenched charge disorder. In fact, the charge fluctuations in the annealed case tend
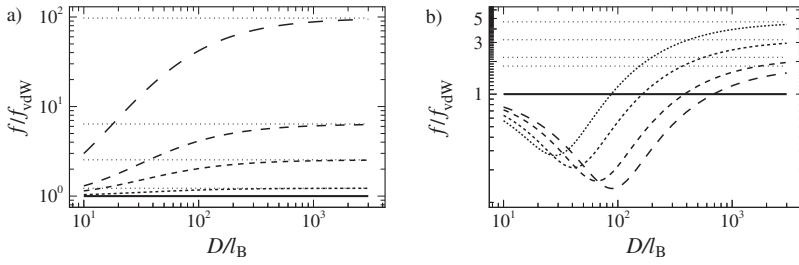
FIG. 4. (a) Same as Fig. 3(a) but here we fix $\varepsilon_p=50$, $g_s=0$, $g_b=5\times10^{-8}$ nm^{-3}, and $\xi=0$ and vary the dielectric constant of the intervening medium as $\varepsilon_m=2$, 10, 20, and 40 (from bottom to top). (b) Same as (a) but here we fix the dielectric constant of the slab as $\varepsilon_p=10$ and vary that of the intervening medium as $\varepsilon_m=30$, 40, 60, and 80 (from top to bottom). Top dotted lines correspond to Eq. (37).

to induce interaction forces that, on the leading order, behave in a dipolar form (decaying as $\sim 1/D^3$ with the distance)—just as one would expect for the case where the slabs are simply composed of free (mobile) positive and negative charges as discussed previously in Sec. III B. This is fundamentally different from the monopolarlike interaction forces obtained, on the leading order, between the slabs carrying quenched charge disorder (Sec. IV A).

In the annealed case, the disorder correlations play a similar role as in the quenched case and tend to weaken the disorder-induced forces. As seen in Fig. 3(a), the magnitude of the force drops from its value for an uncorrelated disorder ($\xi=0$), and also the crossover between the two limiting behaviors as discussed above is "delayed" when the disorder has a finite correlation length, ξ.

It is also remarkable to note that Eq. (37) is obtained in general as the large-distance ($D\rightarrow\infty$) behavior for the total force between any two *arbitrary* dielectric slabs regardless of their dielectric constant and disorder variance. It thus demonstrates the intuitive fact that dielectric slabs with annealed charges tend to behave asymptotically in a way similar to perfect conductors. This is one of the distinctive features of the annealed disorder as compared with the quenched disorder, whose effects depend significantly on the material properties. The deviations due to material properties and the disorder variance in the annealed case contribute a repulsive subleading force in the symmetric case, which can be determined from a series expansion at large separations. If the surface disorder is negligible as compared with the bulk disorder ($g_s\ll g_b\ell_B$), we obtain (up to the first few leading orders)

$$\frac{\beta f_{\text{annealed}}}{S} \simeq -\frac{\zeta(3)}{8\pi D^3} + \frac{3\varepsilon_m\zeta(3)}{\sqrt{64\pi^3 g_b\ell_B\varepsilon_p}D^4} - \frac{3\varepsilon_m^2\zeta(3)}{8\pi^2 g_b\ell_B\varepsilon_p D^5}$$
$$+ \frac{15\xi^2\varepsilon_m\zeta(5)}{2\sqrt{64\pi^3 g_b\ell_B\varepsilon_p}D^6} - \frac{45\xi^2\varepsilon_m^2\zeta(5)}{16\pi^2 g_b\ell_B\varepsilon_p D^7}. \quad (39)$$

While in the opposite situation where the bulk disorder is negligible ($g_s\gg g_b\ell_B$), we obtain

$$\frac{\beta f_{\text{annealed}}}{S} \simeq -\frac{\zeta(3)}{8\pi D^3} + \frac{3\varepsilon_m\zeta(3)}{16\pi^2 g_s\ell_B D^4} + \frac{15\varepsilon_m\xi^2\zeta(5)}{16\pi^2\ell_B g_s D^6}.$$
$$(40)$$

We should emphasize that although the annealed force decays at large separations in a similar fashion as the pure vdW force, its magnitude can nevertheless exceed the vdW force by a few orders of magnitude if the dielectric constant of the intervening material ε_m is increased toward that of the slabs [see Fig. 4(a)]. The asymptotic behavior of the an-

nealed force is similarly described by the pure vdW result (34) and the ideal expression (37) even if the dielectric constant of the (identical) slabs is smaller than that of the intervening medium, $\Delta<0$. However, in this case, these two limiting results do not constitute the upper and lower bound limits for the total force as the force ratio f/f_{vdW} exhibits a nonmonotonic behavior with a local minimum at some intermediate separation between the slabs [Fig. 4(b)].

The special case of a dielectrically homogeneous system, $\varepsilon_1=\varepsilon_2=\varepsilon_m$, constitutes another example where annealed and quenched disorder effects differ on a qualitative level and may thus be easily distinguished. In this case, the total force (25) due to quenched disorder vanishes trivially at all separations, while the total force due to annealed disorder remains finite. Since the vdW contribution vanishes in a dielectrically homogeneous system as well, the total force in this case comes purely from the electrostatic interactions of annealed charges in the two slabs (Fig. 5).

V. ASYMMETRIC CASE OF TWO DISSIMILAR SLABS

So far, we have considered only the case of a symmetric system composed of two identical semi-infinite slabs. In practice, however, one may often deal with a situation where the dielectric constant or disorder variance of the two slabs is different. In this case, the resulting fluctuation-induced interactions may exhibit qualitatively different features as compared with the fully symmetric case that we shall explore further in this section.
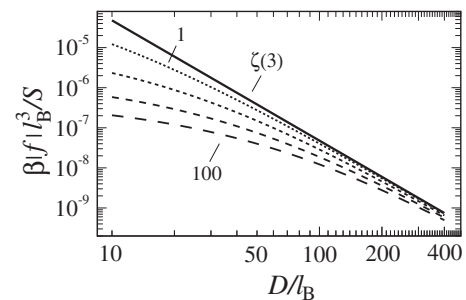

FIG. 5. The rescaled magnitude of the (attractive) force, Eq. (30), between two identical net-neutral dielectric slabs bearing annealed monopolar charge disorder in a *dielectrically homogeneous* system ($\varepsilon_1=\varepsilon_2=\varepsilon_m$) as a function of the rescaled distance, D/l_B. Here we plot the resulting force for $\varepsilon_1=\varepsilon_2=\varepsilon_m=1$, 10, 40, and 100 (from top to bottom) and for uncorrelated bulk disorder in both slabs with $\xi=0$, $g_b=5\times10^{-8}$ nm^{-3}, and $g_s=0$. Top solid line shows the universal limiting expression (37).
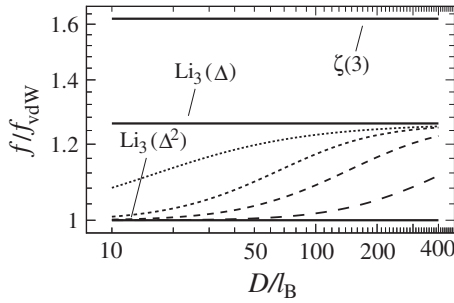
FIG. 6. Same as Fig. 3(a) but for two dissimilar dielectric slabs in vacuum ($\varepsilon_m = 1$) with one slab being disorder free ($g_{1b}, g_{1s} = 0$, $\xi_1 = 0$) and the other slab containing annealed charge disorder of variance $g_{2b} = 5 \times 10^{-8}$ nm^{-3}, $g_{2s} = 0$. Here, we fix $\varepsilon_p = 10$ and vary the disorder correlation length as $\xi_2/l_B = 0$, 200, 10^3, and 10^4 (from top to bottom). The results in this case are bounded by the limiting values given by Eqs. (34) and (42) [solid lines labeled by Li$_3(\Delta^2)$ and Li$_3(\Delta)$, respectively]; see Eq. (41). The top solid line [labeled by $\zeta(3)$] is from Eq. (37).

A. Interaction between a disordered and a disorder free slab

Let us first consider briefly the situation where the two slabs are dielectrically identical, $\varepsilon_1 = \varepsilon_2$ ($\Delta_1 = \Delta_2 = \Delta$), but bear different degrees of quenched or annealed monopolar charge disorder. For the sake of simplicity, let us assume that one slab is *disorder free* ($g_{1b}, g_{1s} = 0$ and $\xi_1 = 0$), whereas the other slab contains disorder charges of bulk and surface variance g_{2b} and g_{2s} and correlation lengths $\xi_{2b} = \xi_{2s} = \xi_2$ (recall that in any case, the net monopolar charge in each slab is taken to be zero).

This case is particularly interesting because it shows the interconnection between the disorder and the dielectric inhomogeneity in the system. In the quenched case, we find that the disorder contribution to the total force is nonzero (even though one of the slabs does not contain any disorder charges), and is simply given by *half* the value obtained in the fully symmetric case [see Eq. (31)] in the previous section if we set $g_{2b} = g_b$, $g_{2s} = g_s$, and $\xi_2 = \xi$ (the vdW contribution is the same in both cases). This result follows straightforwardly from the general quenched expression (25) or Eq. (A1) (see the Appendix) and again reflects the fact that the quenched contribution is basically due to the interaction of disorder charges with their image charges (as these are the only "charges" with which they are "correlated" across the intervening gap). This is why the disorder forces in the quenched case depend essentially on the dielectric jump across the bounding surfaces as discussed before.

In the annealed case, the disordered dielectric slab tends to behave asymptotically as a perfect conductor, while the disorder free slab behaves as a dielectric material. This lowers the *magnitude* of the maximum net force that can be achieved in this system as compared with the case where both slabs bear annealed charges; the latter case is obviously more favorable thermodynamically as the system can achieve a lower free energy. The net annealed force in vacuum still falls between two well-defined limits as shown in Fig. 6. The two bounding limits are given by

$$|f_{\text{vdW}}| < |f_{\text{annealed}}| < |f_*|, \tag{41}$$

where f_{vdW}, Eq. (34), is obtained in the limit of weak disorder or at small separations, and f_*, defined as

$$\frac{\beta f_*}{S} = -\frac{\text{Li}_3(\Delta)}{8\pi D^3}, \tag{42}$$

is obtained in the limit of strong disorder or large separation. Thus, in marked contrast with the fully symmetric case, we find that the large-distance interaction here becomes nonuniversal and could be either attractive ($\Delta > 0$) or repulsive ($\Delta < 0$). This points to the possibility of *repulsive* total forces in the annealed case that will be discussed in the following section.

B. Nonmonotonic interaction between dissimilar slabs with $\varepsilon_1 < \varepsilon_m < \varepsilon_2$

It is clear that the vdW force (18) becomes repulsive when the dielectric constant of the intervening medium is between that of the two semi-infinite slabs, i.e., $\varepsilon_1 < \varepsilon_m < \varepsilon_2$ (such a case has been investigated experimentally in Ref. 15). However, in this case, the force stemming from the quenched charge disorder can be *attractive* and thus, if present, may compete against the repulsion due to the vdW forces. In order to investigate this situation further, let us first consider the case of an uncorrelated disorder by setting the disorder correlation lengths equal to zero. Also without loss of generality, we assume that the slabs contain only quenched bulk disorder with equal variances $g_{1b} = g_{2b} = g_b$ in the two slabs. The net quenched force in this case reads

$$\frac{\beta f_{\text{quenched}}}{S} = -\frac{\text{Li}_3(\Delta_1 \Delta_2)}{8\pi D^3} - \frac{g_b \ell_B \chi}{2(\varepsilon_1 + \varepsilon_2)D}, \tag{43}$$

where we have defined

$$\chi = \frac{(\varepsilon_1 - \varepsilon_m)}{\varepsilon_2 + \varepsilon_m} + \frac{(\varepsilon_2 - \varepsilon_m)}{\varepsilon_1 + \varepsilon_m}. \tag{44}$$

Obviously, the contribution from bulk disorder [second term in Eq. (43)] can change sign as the dielectric constant ε_m is varied in the range $\varepsilon_1 < \varepsilon_m < \varepsilon_2$, while the vdW term (first term) remains always repulsive. It is easy to see that for $\varepsilon_m \to \varepsilon_1$, we have $\chi > 0$ and thus an attractive disorder force, and for $\varepsilon_m \to \varepsilon_2$, we have $\chi < 0$ and thus a repulsive disorder force. This behavior is shown in Fig. 7(a), where $\varepsilon_1 = 5$ and $\varepsilon_2 = 50$ are fixed and ε_m varies in the range $\varepsilon_m = 10$, 15, 25, and 40 (dashed curves from bottom). In accordance with our findings in the symmetric case, the large-distance behavior is always dominated by the disorder contribution (as the disorder force decays more weakly with the separation), while the repulsive vdW force in this case plays the role of a stabilizing force at small separations.

The resulting effect is that the total force varies *nonmonotonically* and vanishes at a finite distance, D_0, between the two slabs given in the present case by

$$D_0^2 = -\frac{\text{Li}_3(\Delta_1 \Delta_2)}{4\pi g_b \ell_B \chi}(\varepsilon_1 + \varepsilon_2). \tag{45}$$

This represents a stable "equilibrium" separation (bound state) between the two slabs corresponding to a minimum in the interaction free energy. On the other hand, the maximum attractive force due to the influence of quenched disorder is reached at a larger separation,
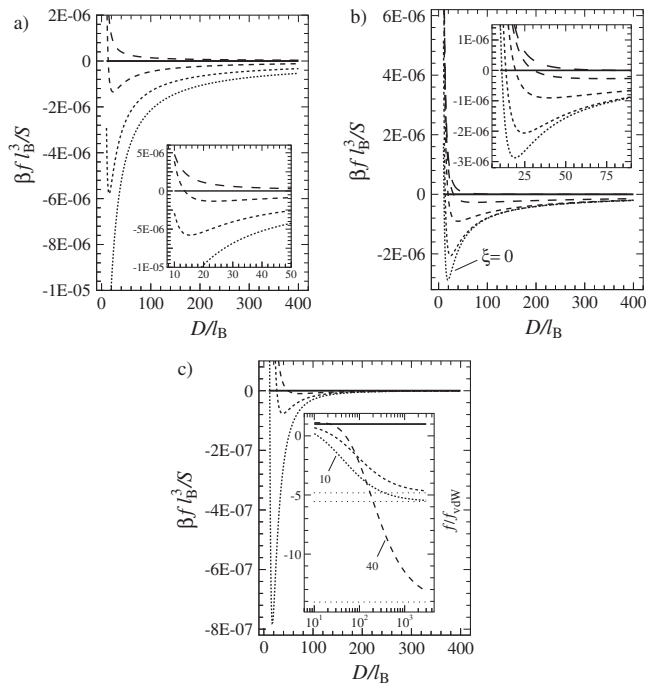
FIG. 7. (a) The rescaled total force, $\beta f l_B^3 / S$ [Eq. (25)], between two dissimilar net-neutral dielectric slabs interacting across a medium of dielectric constant ε_m varying in the range $\varepsilon_m = 10, 15, 25$, and 40 (dashed curves from bottom). Here, we have fixed the dielectric constant of the slabs as $\varepsilon_1 = 5$ and $\varepsilon_2 = 50$, which contain uncorrelated quenched disorder ($\xi_1 = \xi_2 = 0$) of fixed disorder variances $g_{1b} = g_{2b} = 5 \times 10^{-8}$ nm^{-3} and $g_{1s} = g_{2s} = 0$. Inset shows a closer view of the region around the minimum. (b) Same as (a) but plotted for correlated quenched disorder. Here, we fix $\varepsilon_m = 20$ and vary the correlation length as $\xi / l_B = 0, 20, 100, 500$, and 10^4, which is taken to be equal in both slabs $\xi_1 = \xi_2 = \xi$. Inset again shows a closer view of the region around the minimum. (c) Same as (a) but for (uncorrelated) annealed disorder obtained from Eq. (30) for $\varepsilon_m = 10, 20$, and 40. Inset shows the ratio of the total force to the pure zero-frequency vdW force (18) in the absence of charge disorder for a wider range of separations. The horizontal dotted lines show the limiting expression (37).
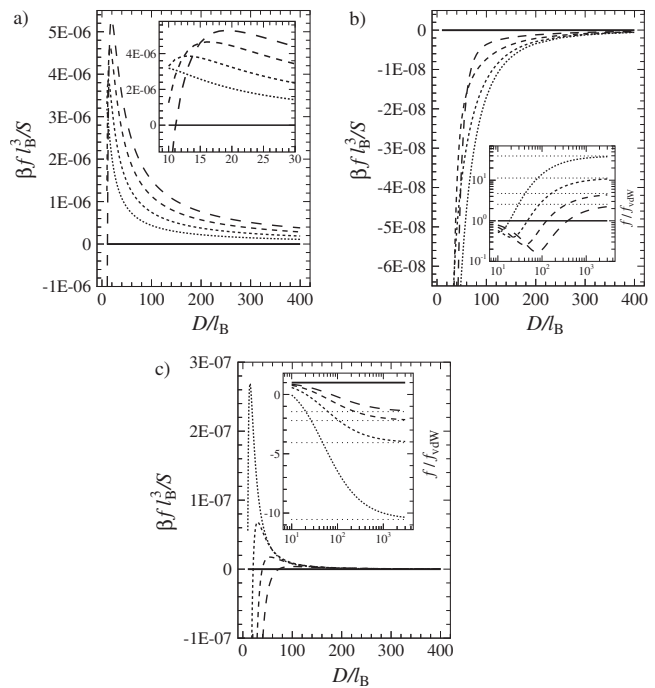
FIG. 8. (a) The rescaled total force, $\beta f l_B^3 / S$ [Eq. (25)], between two dissimilar net-neutral dielectric slabs interacting across a medium of dielectric constant ε_m varying in the range $\varepsilon_m = 30, 40, 60$, and 100 (dashed curves from bottom). Here, we have fixed the dielectric constant of the slabs as $\varepsilon_1 = 15$ and $\varepsilon_2 = 25$, which contain uncorrelated quenched disorder ($\xi_1 = \xi_2 = 0$) of fixed disorder variances $g_{1b} = g_{2b} = 5 \times 10^{-8}$ nm^{-3} and $g_{1s} = g_{2s} = 0$. Inset shows a closer view of the region around the maximum. (b) Same as (a) but for annealed disorder obtained from Eq. (30). Inset shows the ratio of the total force to the vdW force (18) for a wider range of separations; here the horizontal dotted lines correspond to Eq. (37). (c) Same as (a) but for one slab being disorder free ($g_{1b} = g_{1s} = 0$, $\xi_1 = 0$) and the other slab containing annealed charge disorder of variances $g_{2b} = 5 \times 10^{-8}$ nm^{-3} and $g_{2s} = 0$ (dashed curves from top correspond to $\varepsilon_m = 30, 40, 60$, and 100). Inset shows the ratio f / f_{vdW} for a wider range of separations; the horizontal dotted lines correspond to Eq. (42) where Δ should be replaced by Δ_1

$$D_{max} = \sqrt{3} D_0. \tag{46}$$

These results may be used to optimize the thickness of the intervening medium in order to achieve the maximum or minimum force magnitude between the slabs.

In the presence of a correlated disorder, the disorder-induced effects weaken (Sec. IV A), and thus, as the disorder correlation is increased, the attractive tail as well as the stable bound state is gradually washed out as shown in Fig. 7(b).

We find similar features when the disorder charges are annealed as seen in Fig. 7(c). However, in line with our finding in the symmetric case, the net force falls off more rapidly with the separation when the disorder charges are annealed. The large-distance behavior coincides again with the universal expression (37) and can be much larger in magnitude than the pure vdW force (18) when ε_m tends to the larger dielectric constant ε_2 as shown in the inset of Fig. 7(c).

C. Nonmonotonic interaction between dissimilar slabs with $\varepsilon_1, \varepsilon_2 < \varepsilon_m$

In the case where the intervening medium has a higher dielectric constant than the two slabs, $\varepsilon_1, \varepsilon_2 < \varepsilon_m$, the vdW effect leads to an attractive force between the two slabs, Eq. (18), which again dominates at small separations. If the disorder is quenched, the force generated by the disorder can become repulsive and thus lead to a potential barrier and a long repulsive tail at large separations. This is shown in Fig. 8(a), for the case of two slabs with uncorrelated bulk disorder of equal variances ($g_{1b} = g_{2b} = g_b$), where we have fixed $\varepsilon_1 = 15$ and $\varepsilon_2 = 25$ and vary ε_m in the range $\varepsilon_m = 30, 40, 60$, and 100 (dashed curves from bottom). The total force, in this case, is given again by Eq. (43). Note that the disorder-induced force (second term) is always repulsive in the case with $\varepsilon_1, \varepsilon_2 < \varepsilon_m$ (i.e., $\chi < 0$). Thus, the separation distance D_0, Eq. (45), corresponds to an unstable equilibrium distance between the two slabs, and D_{max} gives the distance at which the maximum repulsive force due to the influence of quenched disorder is achieved.

The above features change dramatically if the disorder charges are assumed to be annealed. In fact, the net annealed force appears to follow a trend similar to what one expects from the pure vdW force, i.e., in contrast with the quenched case, the net annealed force turns out to be attractive and vary monotonically with the separation [Fig. 8(b)]. However, the ratio of the net force to the vdW force (18) shows that the relative magnitude of the force can vary nonmonotonically

and deviate significantly from the underlying vdW force [Fig. 8(b), inset]. In particular, one observes that the relative net force may be enhanced here by an order of magnitude at large separations. This is again due to fluctuations of annealed charges that can redistribute in the slabs in such a way as to minimize the free energy and thus favor a higher attractive force.

In the preceding discussion, we assumed that the two slabs have similar annealed disorder variances, which leads to a purely attractive force between the slabs for $\varepsilon_1, \varepsilon_2 < \varepsilon_m$. It turns out that the annealed disorder can also lead to a repulsive force in this case, provided that the charge is distributed asymmetrically between the two slabs. In Fig. 8(c), we show the results for the case where one of the slabs is disorder free, but the other slab contains annealed charge disorder of finite variance. As seen, one can achieve an interaction (potential) barrier even with the annealed charges. This effect is stronger when ε_m is smallest and disappears when $\varepsilon_m \rightarrow \infty$.

VI. DISCUSSION

In this paper, we have shown that the effective interaction induced by the quenched or annealed monopolar charge disorder can give rise to various novel features in the overall interaction between two net-neutral semi-infinite dielectric slabs depending on the detailed assumptions about the disorder and the dielectric inhomogeneities in the system. The quenched case and the annealed case of disorder differ in the sense that in the former the disordered charges are frozen and cannot fluctuate, while in the latter, the disordered charges are subject to thermal fluctuations and adapt themselves to minimize the free energy of the system. Our analysis is based on recent developments, which unify the salient features of the zero-frequency vdW interaction and the physics of the charge disorder.[8,12,13] Based on these developments, we argue that in the case of two dissimilar slabs, the charge disorder-induced electrostatic interaction can have an opposite sign to the zero-frequency vdW interaction and can thus give rise to a nonmonotonic net interaction between the slabs. The most surprising features of our analysis pertain to the case of disorder-induced interactions across a medium of higher dielectric constant than that of the two slabs. In this case, the net force may become strongly repulsive and can lead to a potential barrier for stiction when combined with the attractive vdW force. In the opposite case, where the intervening medium has a dielectric constant in between that of the two slabs, the disorder may generate a long-range attraction, which opposes the repulsive vdW force and can thus promote a stable bound state for the two bounding dielectrics. These salient features of the disorder-induced interactions are due to the slower decay of these interactions and their stronger dependence on the dielectric inhomogeneities in the system as compared to the corresponding vdW interaction.

This comparison between the disorder-induced and the classical zero-frequency vdW interaction is in order since both of them are expected to be valid in the regime of large intersurface separations (or high temperatures) as considered

in this work and that is also most relevant to recent experiments.[6] The precise correction presented by the higher-order Matsubara frequencies[25] is highly material specific, but its magnitude (relative to the zero-frequency term) is typically small for the most part of the separation range considered here and remains negligible in comparison with the disorder effects.

The nonmonotonic interactions predicted within our model emerge in highly asymmetric systems where the slabs and the intervening medium have different dielectric constants. In fact, an experimental investigation of the Casimir-vdW interactions in such systems has been made possible recently,[15] which could facilitate the study of possible disorder-induced effects in these systems as well. On the other hand, recent ultrahigh sensitivity experiments *in vacuo* have revealed the existence of long-range anomalous forces that have been related to electrostatic disorder effects.[6] For the experimental *sphere-plane* geometry,[6] a naive application of the *proximity force approximation*[5] to the results derived above for uncorrelated disorder would lead to forces with the leading behavior $\sim \ln D + \mathcal{O}(D^{-1})$ in the quenched case [from Eq. (32)] and $\sim D^{-2} + \mathcal{O}(D^{-3})$ in the annealed case [from Eqs. (39) and (40)]. Thus, an effective scaling exponent (defined as $D^{-\alpha}$) of $\alpha \leq 1$ (consistent with recent experimental observation[6] of a residual electrostatic force scaling as $D^{-0.8}$) may be obtained in the quenched case, both with the bulk disorder (plane-plane and sphere-plane geometry) and the surface disorder model (sphere-plane geometry) in the regime where the disorder correlation length is relatively small. A more detailed comparison with force measurements should be attempted once the experimental and methodological uncertainties surrounding experiments are sorted out.[6]

In general, the impurities carrying the monopolar charge disorder can make contributions to the dielectric constant of the material through their intrinsic polarizability. This may renormalize the dielectric constant, but otherwise, the general expressions we have obtained remain intact. It should be noted, however, that the density of such impurity charges is very small in many realistic situations relevant to our study, and we have consistently used disorder concentration of (much) less than $10^{-7}\ e_0/\mathrm{nm}^3$ throughout the paper.[24] The charge disorder effects are still considerable at these concentrations, but any renormalization of the dielectric constant will be negligible.

Being disorder-induced, one should be in principle also able to compute the corresponding statistical moments of the disorder-induced forces averaged over the disorder realizations.[26] Note that these fluctuations over the disorder will be different from the thermal fluctuations of the Casimir force studied in Ref. 27, which are present even in the absence of disorder.

ACKNOWLEDGMENTS

neering, and the British Academy. J.S. acknowledges generous support by J. Stefan Institute (Ljubljana) provided for a visit to the Institute.

APPENDIX: GENERAL EXPRESSION FOR THE FORCE IN THE QUENCHED CASE

In the general case where the two slabs (labeled by $i = 1, 2$) have different dielectric constants and charge disorder parameters, we can write the total force, Eq. (25), as a series expansion in powers of $\xi_{i\alpha}/D$ (for the bulk and surface disorder, $\alpha = b, s$), i.e.,

$$f_{\text{quenched}} = f^{(0)} + \sum_{n=1}^{\infty} (f_1^{(n)} + f_2^{(n)}), \tag{A1}$$

where we obtain

$$\frac{\beta f^{(0)}}{S} = -\frac{g_{1b}\ell_B(\varepsilon_2 + \varepsilon_m)\Delta_2}{2(\varepsilon_1 + \varepsilon_m)(\varepsilon_1 + \varepsilon_2)D} - \frac{g_{1s}\ell_B\varepsilon_m|\ln(1 - \Delta_1\Delta_2)|}{(\varepsilon_1 + \varepsilon_m)^2\Delta_1 D^2}$$
$$- \frac{g_{2b}\ell_B(\varepsilon_1 + \varepsilon_m)\Delta_1}{2(\varepsilon_2 + \varepsilon_m)(\varepsilon_1 + \varepsilon_2)D} - \frac{g_{2s}\ell_B\varepsilon_m|\ln(1 - \Delta_1\Delta_2)|}{(\varepsilon_2 + \varepsilon_m)^2\Delta_2 D^2} \tag{A2}$$

and

$$\frac{\beta f_1^{(n)}}{S} = -\frac{2g_{1b}\ell_B\varepsilon_m}{(\varepsilon_1 + \varepsilon_m)^2\Delta_1 D}\sum_{n=1}^{\infty}(-1)^n\frac{\xi_1^{2n}}{D^{2n}}C_{2n+1}\text{Li}_{2n}(\Delta_1\Delta_2)$$
$$- \frac{4g_{1s}\ell_B\varepsilon_m}{(\varepsilon_1 + \varepsilon_m)^2\Delta_1 D^2}\sum_{n=1}^{\infty}(-1)^n\frac{\xi_1^{2n}}{D^{2n}}C_{2n+2}\text{Li}_{2n+1}(\Delta_1\Delta_2), \tag{A3}$$

where $C_n = \Gamma(n)/2^n$. The expression for $f_2^{(n)}$ is obtained simply by replacing the subindex 1 with 2 and vice versa.

[1] E. J. W. Verwey and J. Th. G. Overbeek, *Theory of the Stability of Lyophobic Colloids* (Elsevier, Amsterdam, 1948); J. N. Israelachvili, *Intermolecular and Surface Forces* (Academic, London, 1990).

[2] E. E. Meyer, Q. Lin, T. Hassenkam, E. Oroudjev, and J. N. Israelachvili, Proc. Natl. Acad. Sci. U.S.A. **102**, 6839 (2005); S. Perkin, N. Kampf, and J. Klein, Phys. Rev. Lett. **96**, 038301 (2006); J. Phys. Chem. B **109**, 3832 (2005); E. E. Meyer, K. J. Rosenberg, and J. Israelachvili, Proc. Natl. Acad. Sci. U.S.A. **103**, 15739 (2006).

[3] Y. Kantor, H. Li, and M. Kardar, Phys. Rev. Lett. **69**, 61 (1992); I. Borukhov, D. Andelman, and H. Orland, Eur. Phys. J. B **5**, 869 (1998).

[4] B. W. Ninham and V. A. Parsegian, J. Theor. Biol. **31**, 405 (1971).

[5] M. Bordag, G. L. Klimchitskaya, U. Mohideen, and V. M. Mostepanenko, *Advances in the Casimir Effect* (Oxford University Press, New York, 2009).

[6] W. J. Kim, M. Brown-Hayes, D. A. R. Dalvit, J. H. Brownell, and R. Onofrio, Phys. Rev. A **78**, 020101(R) (2008); **79**, 026102 (2009); W. J. Kim, A. O. Sushkov, D. A. R. Dalvit, and S. K. Lamoreaux, Phys. Rev. Lett. **103**, 060401 (2009); R. S. Decca, E. Fischbach, G. L. Klim-

chitskaya, D. E. Krause, D. López, U. Mohideen, and V. M. Mostepanenko, Phys. Rev. A **79**, 026101 (2009); S. de Man, K. Heeck, and D. Iannuzzi, *ibid.* **79**, 024102 (2009).

[7] C. C. Speake and C. Trenkel, Phys. Rev. Lett. **90**, 160403 (2003).

[8] A. Naji, D. S. Dean, J. Sarabadani, R. R. Horgan, and R. Podgornik, Phys. Rev. Lett. **104**, 060601 (2010).

[9] L. F. Zagonel, N. Barrett, O. Renault, A. Bailly, M. Bäurer, M. Hoffmann, S.-J. Shih, and D. Cockayne, Surf. Interface Anal. **40**, 1709 (2008).

[10] Z. H. Liu, N. M. D. Brown, and A. McKinley, J. Phys.: Condens. Matter **9**, 59 (1997).

[11] D. S. Dean, R. R. Horgan, A. Naji, and R. Podgornik, Phys. Rev. A **79**, 040101(R) (2009); Phys. Rev. E **81**, 051117 (2010).

[12] A. Naji and R. Podgornik, Phys. Rev. E **72**, 041402 (2005); R. Podgornik and A. Naji, Europhys. Lett. **74**, 712 (2006).

[13] Y. S. Mamasakhlisov, A. Naji, and R. Podgornik, J. Stat. Phys. **133**, 659 (2008).

[14] A. Naji *et al.* (unpublished).

[15] J. N. Munday, F. Capasso, and V. A. Parsegian, Nature (London) **457**, 170 (2009).

[16] The Gaussianity assumption is unimportant for quenched charges, and only the correlation function $\langle\langle \rho(\mathbf{r})\rho(\mathbf{r}')\rangle\rangle$ needs to be given.

[17] Our model for the correlation function in Eq. (8) implies isolated patches of positive and negative charges. It is worth mentioning that this form of the charge density correlation function may be obtained for a plasma of negative and positive charges only if an underlying non-Coulombic interaction is present between the ions with, e.g., impurities that induce such correlations in the distribution of the ions. In fact, for a *free* plasma of mobile ions at equilibrium, the charge density correlation function in the Debye–Hückel limit takes a different form, which can be expressed in the Fourier representation as $c_{i\alpha}^{\text{DH}}(Q) = \xi_{i\alpha}^2 Q^2/(\xi_{i\alpha}^2 Q^2 + 1)$. Such a model for the charge correlation function is not an example of the patchy charge distribution we consider here [compare with Eq. (24)]. In other words, the patchiness in charge distribution is absent in a fully equilibrated Debye–Hückel plasma of free positive and negative ions interacting solely via the Coulomb potential; this is due to the effect of screening.

[18] V. Dotsenko, *Introduction to the Replica Theory of Disordered Statistical Systems* (Cambridge University Press, New York, 2001).

[19] R. Podgornik, J. Chem. Phys. **91**, 5840 (1989).

[20] J. Mahanty and B. W. Ninham, *Dispersion Forces* (Academic, London, 1976).

[21] R. Podgornik, Chem. Phys. Lett. **144**, 503 (1988).

[22] J. S. Høye and I. Brevik, Phys. Rev. E **80**, 011104 (2009); B. Jancovici and L. Šamaj, J. Stat. Mech.: Theory Exp. 2004, P08006.

[23] If we were to construct a quenched model by freezing equilibrium configurations of a Debye–Hückel plasma as noted above (Ref. 17), the behavior of the quenched interaction force would be purely dipolar to leading order [rather than being monopolar with dipolar corrections as we obtain in Eq. (31) for our current model]. This is because the Debye–Hückel correlation function (Ref. 17), c^{DH}, differs from the present correlation function (24) in that it behaves as $\sim Q^2$ in the limits $\xi_{i\alpha}$ and/or $Q \to 0$ and thus yields the leading quenched force behavior as $\sim 1/D^3$ for the bulk disorder and $\sim 1/D^4$ for the surface disorder.

[24] K. C. Kao *Dielectric Phenomena in Solids* (Elsevier Academic, San Diego, 2004); L. P. Pitaevskii, Phys. Rev. Lett. **101**, 163202 (2008).

[25] V. A. Parsegian, *Van der Waals Forces* (Cambridge University Press, 2005).

[26] D. S. Dean, A. Naji, and R. Podgornik, "Sample-to-sample fluctuations of electrostatic forces generated by quenched charge disorder," http://arxiv.org/abs/1009.4032.

[27] D. Bartolo, A. Ajdari, J. B. Fournier, and R. Golestanian, Phys. Rev. Lett. **89**, 230601 (2002).